CFD SIMULATION AND ANN PREDICTION OF HYDROGEN LEAKAGE AND DIFFUSION BEHAVIOR IN A HYDROGEN REFUELLING STATION

Li, Y.Z.[1], Xu, N.F[1], Liu, M.[2], Tong, L.[3], Yuan, C.Q.[3], Yang, T.Q.[1, *], Li, X.F.[4] and Xiao, J.S.[1, 4]

[1] Hubei Research Center for New Energy & Intelligent Connected Vehicle and Hubei Key Laboratory of Advanced Technology for Automotive Components, School of Automotive Engineering, Wuhan University of Technology, Hubei 430070, China, liyaze1998@whut.edu.cn, xnf@sae-china.org, tqyang@whut.edu.cn, jsxiao@whut.edu.cn
[2] Research Institute of State Grid Zhejiang Electric Power CO., LTD. Hangzhou, 310006, China, liumhb@126.com
[3] School of Transportation and Logistics Engineering, Wuhan University of Technology, Hubei, 430070, China, tongliang2@whut.edu.cn, ycq@whut.edu.cn
[4] Institute of Thermal Science and Technology, Shandong University, Shandong 250061, China, lixf@email.sdu.edu.cn, jsxiao@whut.edu.cn

ABSTRACT

Hydrogen refuelling stations are an important part of the infrastructure for promoting the hydrogen economy. Since hydrogen is a flammable and explosive gas, hydrogen released from high-pressure hydrogen storage equipment in hydrogen refuelling stations will likely cause combustion or explosion accidents. Studying high-pressure hydrogen leakage in hydrogen refuelling stations is a prerequisite for promoting hydrogen fuel cell vehicles and hydrogen refuelling stations. In this work, an actual-size hydrogen refuelling station model was established on the ANSYS FLUENT software platform. The computational fluid dynamics (CFD) models for hydrogen leakage simulation were validated by comparing the simulation results with experimental data in the literature. The effects of ambient wind speed, wind direction, leakage rate and leakage direction on the diffusion behaviors of the released hydrogen were investigated. The spreading distances of the flammable hydrogen cloud were predicted using an artificial neural network for horizontal leakage. The results show that the leak direction strongly affected the flammable cloud flow. The ambient wind speed has complicated effects on spreading the flammable cloud. The wind makes the flammable cloud move in certain directions, and the higher wind speed accelerates the diffusion of the flammable gas in the air. The results of the study can be used as a reference for the study of high-pressure hydrogen leakage in hydrogen refuelling stations.

1. INTRODUCTION

Hydrogen energy is a safe and environmentally friendly energy carrier with a wide range of sources and has shown great application value in the energy field. The most typical application of hydrogen energy is for hydrogen fuel cell vehicles. Compared with the long-time charging of traditional rechargeable vehicles, fuel cell vehicles can be refueled with hydrogen through hydrogen refuelling stations, similar to fuel cars, which have the advantages of fast fuel refuelling and long range. The continuous rise of these new technologies also brings great opportunities to the hydrogen energy industry.

As a necessary infrastructure for the commercialization of fuel cell vehicles, hydrogen refuelling stations have received high priority from governments worldwide. One of the biggest challenges is the safety issues caused by the inherent properties of hydrogen, including low density, a wide range of flammability and a low minimum ignition rate. In case of hydrogen leakage, hydrogen energy-related accidents can be easily caused due to the inherent characteristics of hydrogen. Therefore, researchers have studied the diffusion of hydrogen leaks in different environments. Literatures [1-5] are studies on hydrogen leakage and diffusion behavior in open space. Literatures [1,2] mainly used FLUENT to simulate the process of hydrogen leakage and diffusion in open space and conducted parameter research. Literatures [3,4] used FLACS to study the range of ignition and explosion accidents after hydrogen leakage. Literature [5] is mainly on the hydrogen storage system by using the method of accident tree common hazards are analyzed. Literatures [6-10] study hydrogen leakage and diffusion behavior in a limited space. Literatures [6-7] mainly established two different hydrogen diffusion models in limited

space through theoretical and experimental methods: the Filling box model and Fading up box model. Literatures [8,9] are some experiments on hydrogen leakage diffusion in limited space, and the experimental results are used to analyze the hydrogen distribution in limited space. In the literature [10], three scenarios were simulated numerically: immediate ignition after a high-pressure hydrogen leak, delayed ignition, and delayed ignition in the presence of a protective wall.

This study established a simplified three-dimensional model of the hydrogen refuelling station based on a proposed hydrogen refuelling station in China. The research focused on the horizontal leakage of the 45MPa hydrogen storage tank in the hydrogen storage area. The effects of mass flow rate of hydrogen leakage, ambient wind direction and ambient wind speed on hydrogen dispersion behavior were investigated in this case. An artificial neural network was used to predict the dispersion distance and provide suggestions for reducing the risk of hydrogen leakage accidents.

2. INTRODUCTION OF MODEL AND SIMULATION

2.1 FUNDAMENTAL GOVERNING EQUATION AND TURBULENCE MODEL

The basic governing equations for hydrogen diffusion in the air include mass, momentum and energy conservations and component transport equation. The mass conservation equation can be expressed as:

$$\frac{\partial \rho}{\partial t} + \nabla \cdot (\rho \boldsymbol{u}) = 0 \tag{1}$$

where ρ – density of hydrogen, kg/m³; t – time, s; $\boldsymbol{u}$ – the velocity vector, m/s.

The momentum conservation equation can be expressed as:

$$\frac{\partial}{\partial t}(\rho \boldsymbol{u}) + \nabla \cdot (\rho u \boldsymbol{u}) = -\nabla p + \nabla \cdot \bar{\tau} + \boldsymbol{F} \tag{2}$$

where p – pressure, Pa; $\bar{\tau}$ – stress tensor, Pa; $\boldsymbol{u}$ – velocity vector, m/s; $\boldsymbol{F}$ –the body force, N.

The energy conservation equation can be expressed as:

$$\frac{\partial(\rho c_p T)}{\partial t} + \nabla \cdot \left(\rho c_p \boldsymbol{u} T\right) = \frac{\partial}{\partial x}\left(k\frac{\partial T}{\partial x}\right) + \frac{\partial}{\partial y}\left(k\frac{\partial T}{\partial y}\right) + \frac{\partial}{\partial z}\left(k\frac{\partial T}{\partial z}\right) + \phi + S_h \tag{3}$$

where c_p – specific heat capacity at constant pressure, J/(kg·K); T – temperature, K; k – thermal conductivity, W/(m·K); ϕ– dissipation function; S_h– internal heat source in fluid, W/m³.

The component transport equation can be expressed as:

$$\frac{\partial(\rho c_s)}{\partial t} + \nabla \cdot (\rho c_s \boldsymbol{u}) = \frac{\partial}{\partial x}\left(D_s \frac{\partial(\rho c_s)}{\partial x}\right) + \frac{\partial}{\partial y}\left(D_s \frac{\partial(\rho c_s)}{\partial y}\right) + \frac{\partial}{\partial z}\left(D_s \frac{\partial(\rho c_s)}{\partial z}\right) \tag{4}$$

where c_s – volume fraction of component s; D_s – diffusion coefficient of component s in air, m²/s.

The wall function adopts the standard wall function. Standard k- ε Model is selected for the turbulence model in the simulation. The model is a dual equation turbulence model, which allows for the determination of turbulent kinetic energy k and dissipation rate ε by solving two independent transport equations.The equation for turbulent kinetic energy k is as follows:

$$\frac{\partial}{\partial t}(\rho k) + \frac{\partial}{\partial x_i}(\rho k u_i) = \frac{\partial}{\partial x_j}\left[(\mu + \frac{\mu_t}{\sigma_k})\frac{\partial k}{\partial x_j}\right] + G_k + G_b - \rho \varepsilon - Y_M + S_k \tag{5}$$

The equation for dissipation rate ε is as follows:

$$\frac{\partial}{\partial t}(\rho\varepsilon) + \frac{\partial}{\partial x_i}(\rho\varepsilon u_i) = \frac{\partial}{\partial x_j}\left[\left(\mu + \frac{\mu_t}{\sigma_\varepsilon}\right)\frac{\partial\varepsilon}{\partial x_j}\right] + C_{1\varepsilon}\frac{\varepsilon}{k}(G_k + C_{3\varepsilon}G_b) - C_{2\varepsilon}\rho\frac{\varepsilon^2}{k} + S_\varepsilon \tag{6}$$

where σ_k – Turbulent Prandtl number of turbulent kinetic energy; σ_ε – Turbulent Prandtl number of dissipation rate; G_k – turbulent kinetic energy related to average velocity gradient, J; G_b – turbulent kinetic energy related to buoyancy, J; $C_{1\varepsilon}$, $C_{2\varepsilon}$, $C_{3\varepsilon}$ – constant, describing the effect of buoyancy on dissipation rate ε; Y_M – effect of turbulent waves in compressible fluid on dissipation rate ε. Turbulent viscosity μ_t can be calculated based on turbulent kinetic energy k and dissipation rate ε:

$$\mu_t = \rho C_\mu \frac{k^2}{\varepsilon} \tag{7}$$

2.2 VALIDATION OF CFD METHOD FOR HYDROGEN DIFFUSION

In this section, CFD simulations of the experiments conducted by Pitts et al. [9] are presented. The results are compared with the experimental results to verify the feasibility of studying the hydrogen diffusion behavior by CFD methods. The experiment was conducted in a garage with internal dimensions of 6.10 m (L) × 6.10 m (W) × 3.05 m (H).

The experimental condition is that hydrogen gas leaks into the garage at a mass flow rate of 83.3 g/min from a hydrogen release point dispenser (a 15 cm high, 30.5 cm square steel box with an open top) located flush with the ground in the center of the garage, with a leakage time of 3651 s. Three sensors at the coordinates of (3.05,5.49,0.38), (3.05,5.49,1.52) and (3.05, 5.49, 3.05) were used as the monitoring points, which were denoted as M1, M2 and M3. The simulated data at the three locations were compared with the experimental data to verify the feasibility of the CFD method. The meshing of the simulation model based on the experimental garage model is shown in Figure 1(a). The curves of hydrogen volume fraction versus time at three monitoring points M1, M2 and M3 were obtained through simulation, and the results of simulations compared with experimental results are shown in Figure 1(b).
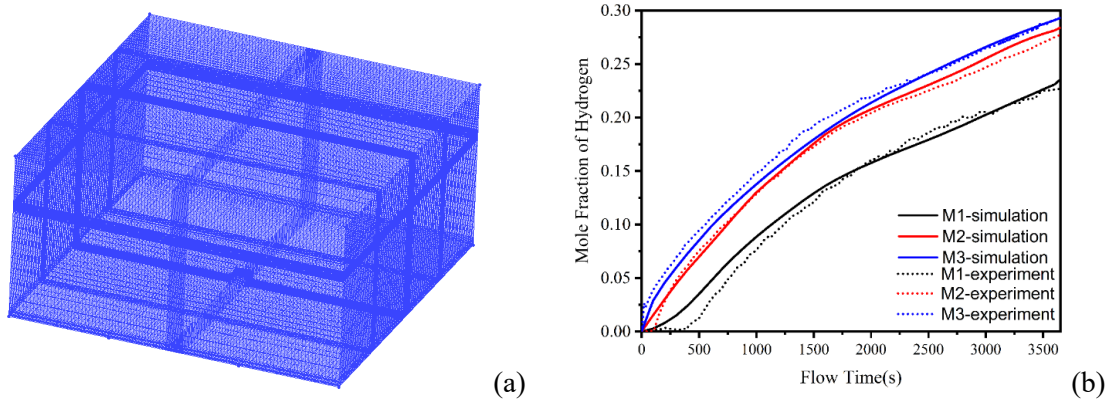

(a)

(b)

Fig.1 Model mesh (a) and comparison of simulation and experimental data (b)

During the process, the maximum relative error was 8.7% for point M1, 6.9% for point M2, and 4.97% for point M3. At the end of the leakage, the simulation result of point M1 was 23.5%, the experimental result was 22.6%, and the relative error was 3.98%. The simulation result of point M2 was 28.4%, the experimental result was 27.7%, and the relative error was 2.53%. The simulation result of point M3 was 29.3%, the experimental result was 29.259%, and the relative error was 0.14%. The analysis shows that the calculated results of the three monitoring points at the early stage of the leakage have some errors with the experimental results and then gradually converge. Still, the overall trend is the same, and the final hydrogen volume fraction is basically the same. The main reasons for the error are as follows. (1) During the modeling process, some simplification was made to the surrounding environment. (2) The initial leakage conditions could not be completely consistent with the actual situation. (3) Different sizes of simulation steps could also cause certain errors. (4) The experimental data was obtained by taking

3

points from the charts published in the paper, which had some differences from the original experimental results, resulting in errors between the final simulation data and the experimental data.

2.3 HYDROGEN REFUELLING STATION MODEL

The hydrogen refuelling station includes the hydrogen production area, the micro-grid control area, the hydrogen storage area and the hydrogen refuelling area. It is assumed that the hydrogen production and micro-grid control areas are closed, and the leaking hydrogen will not enter the two areas.
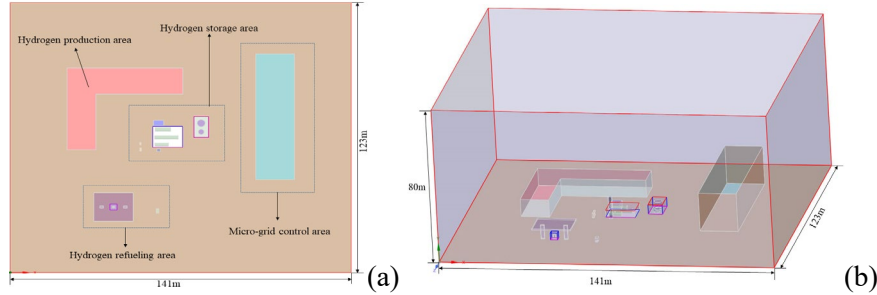

Fig.2 Schematic diagram of (a)hydrogen refuelling station layout and (b)3D simplified model

Figure 2 shows the floor plan of the hydrogen refuelling station and the 3D simplified model created. Considering the wide range of hydrogen leakage in open spaces, the simulation model centers around the hydrogen storage area and extends around it. The final overall calculation domain is a rectangular area with a length of 141 m, a width of 123 m, and a height of 80 m. The colored boxed area in Figure 2(b) is the refined area during mesh division.

2.4 MESHING

Since the shape of each building and equipment in the simplified hydrogen refuelling station is relatively regular, ICEM software was used to construct the external model for meshing. Considering the difficulty of meshing and the number of meshes, the model was divided into different parts, hydrogen refuelling area, hydrogen storage area and air domain, according to the principle of hybrid meshing technology, and the meshes of these parts were divided independently. Finally, the divided meshes are combined by combining the meshes. The common interface between the different areas is set as the interface to correlate the nodes and reduce the influence of different interfaces on the data transfer. The simplified Molkov[11] national nozzle model results in a leakage radius of 111mm, a leakage mass flow rate of 4.5589kg/s, and a temperature of 250K. The specific mesh division results are shown in Figure 3. Due to the formation of high-speed jets at the leakage port during leakage, it is necessary to encrypt the grid near the leakage port to prevent non convergence. The main method is to establish a 12m long, 9.6m wide, and 3m high encryption area around the hydrogen storage tank, as well as a 3m long, 2.6m wide, and 3m high encryption area around the hydrogen refueling machine.

Four grids with different numbers of 4.84, 5.5, 6.5 and 7.5 million were plotted for the grid-independent analysis. The simulation was performed to verify the grid independence with the set hydrogen volume fraction at the monitoring points and the overall flammable domain volume parameters. The validation conditions were the leakage of high-pressure hydrogen from the 45MPa hydrogen storage tank in both vertical and horizontal directions and the leakage from the hydrogen refuel machine in the vertical direction at a wind speed of 0m/s simulation time was 10 s. The results are shown in Figure 4. Considering the calculation accuracy and time, 6.5 million grids were finally selected for subsequent simulation calculations. The target mesh size of the face mesh of the leakage port is 10mm, the target mesh size of the body mesh in the encrypted area is 65mm, and the target mesh size of the overall external space volume mesh is 750mm. The mesh growth rate for all area is 1.2. The final mesh number is 650w.
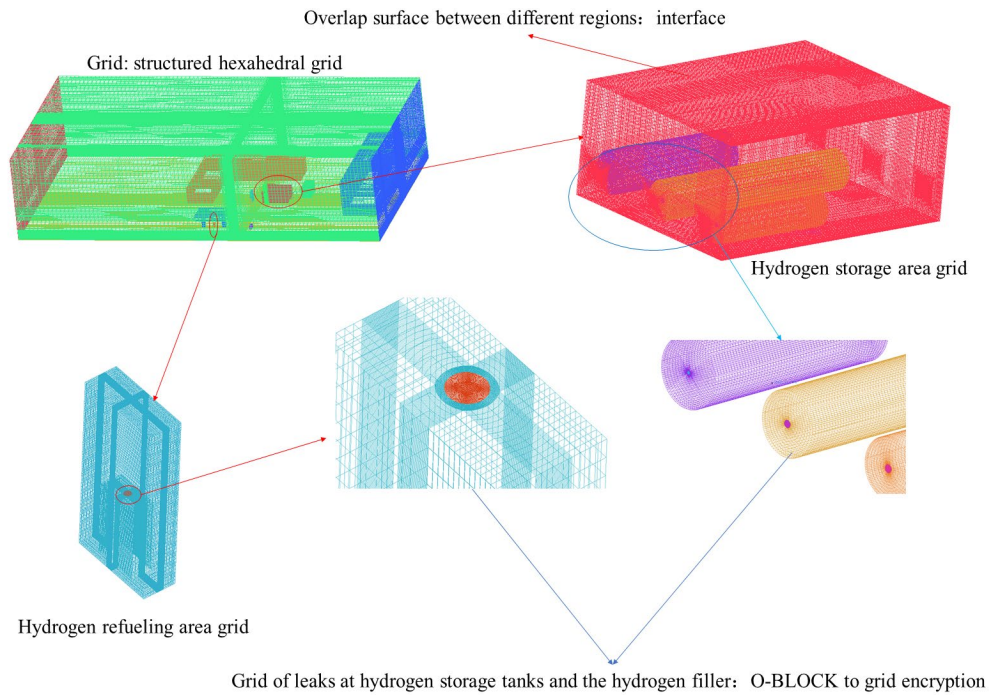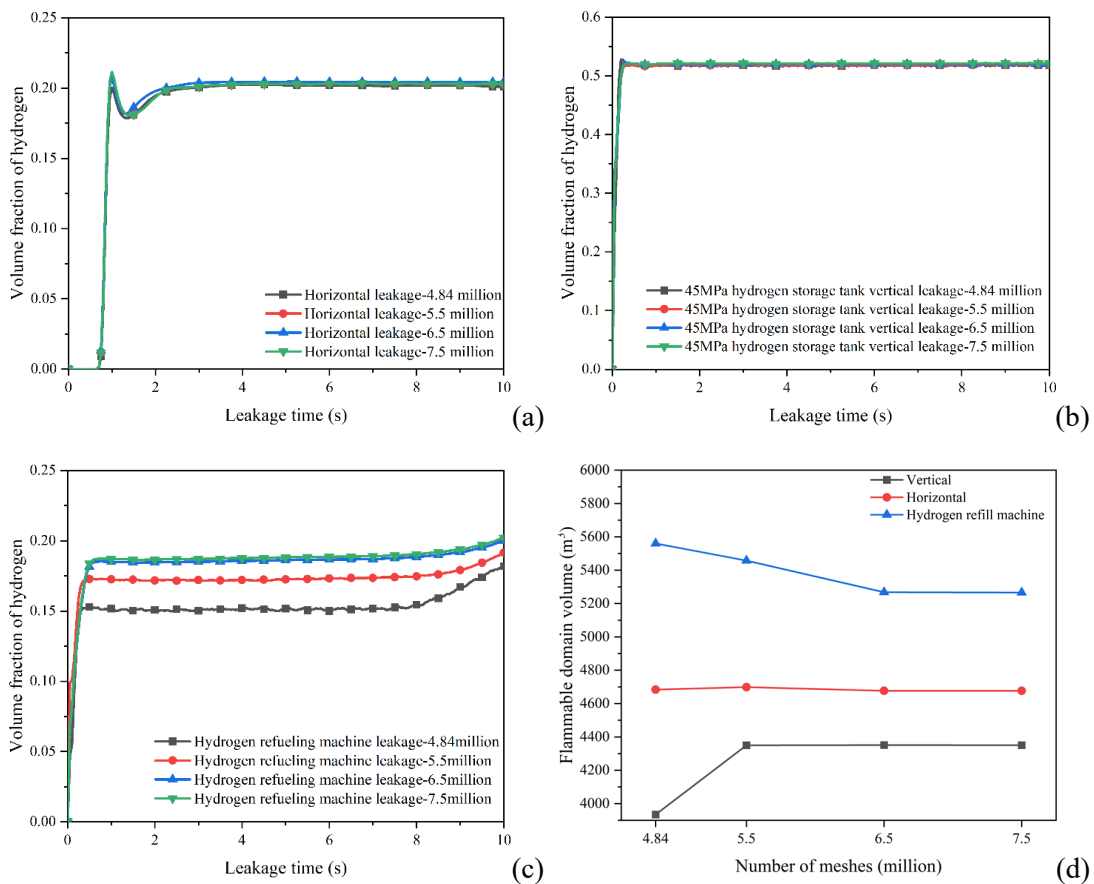
Fig.3 The results of dividing the computational mesh

Fig.4 Comparison of the volume fraction of hydrogen at the monitoring points after the end of leakage of (a) 45MPa hydrogen storage tank horizontal leakage, (b)45MPa hydrogen storage tank vertical leakage, (c) hydrogen refuelling machine, and (d) comparison of the volume of the overall flammable hydrogen cloud at the end of the leak under different mesh numbers

3. STUDY ON PARAMETERS AFFECTING HYDROGEN LEAKAGE AND DIFFUSION BEHAVIOR

3.1 Leakage Direction

This section analyzes the hydrogen diffusion behavior of the 45 MPa hydrogen storage tank when it leaks in different leak directions. The set leakage positions are: Located in the center of the left side of the hydrogen storage tank, with the leakage direction in the horizontal direction; Located in the center of the upper wall of the hydrogen storage tank, the leakage direction is vertical and upward. During the simulation, the ambient wind speed is 0 m/s.

3.1.1 Horizontal leakage of 45MPa hydrogen storage tank

When leakage occurs at the side leakage port of the hydrogen storage tank, high-pressure hydrogen leaks horizontally from the leakage port. Hydrogen diffusion behavior during a leak is analyzed using a time-dependent graph of a flammable hydrogen cloud (areas with a hydrogen volume fraction of 4% to 74%). The specific process is shown in Figure 6.

At the initial leakage stage, hydrogen is emitted horizontally from the leakage port at high speed and diffuses toward the surrounding environment. Due to the ambient wind speed of 0 m/s, no wind speed affects the diffusion speed of hydrogen leakage. Therefore, at the initial stage of leakage, kinetic energy has a greater impact on the diffusion of leakage than buoyancy. As can be seen from the figure, at 0.2 s, hydrogen has diffused to the pressure reduction valve (A 1.26m long, 0.6m wide and 2.08m high cuboid) and wrapped around it. This is because the pressure reduction valve hinders hydrogen diffusion, causing the hydrogen at the pressure reduction valve to be split into two parts. A part of the hydrogen spreads through the left and right sides of the pressure reduction valve. The speed loss of this part of hydrogen is relatively small, mainly due to the change in the speed direction; Another part of hydrogen diffuses to the surface of the pressure reduction valve, resulting in a velocity loss. Eventually, the volume fraction of hydrogen was increased near the pressure reduction valve, and the flammable hydrogen cloud was formed.
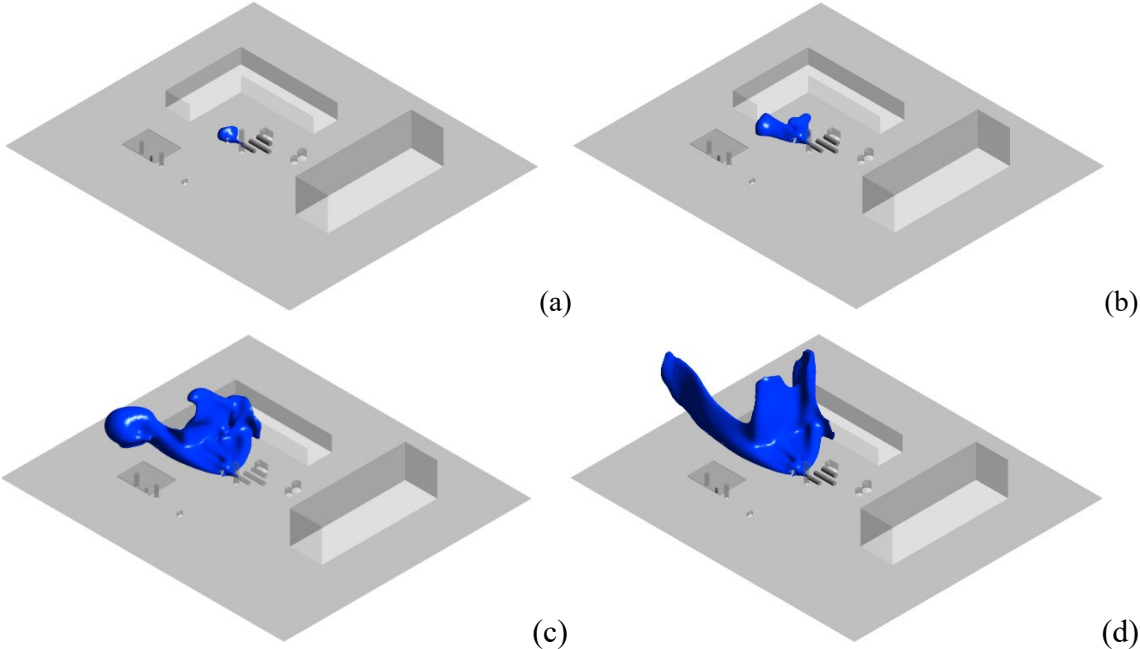

(a)

(b)

(c)

(d)

Fig.6 The distribution range of flammable hydrogen cloud when the horizontal leakage time is (a) 0.2s, (b) 1s, (c) 10s and (d) 30s.
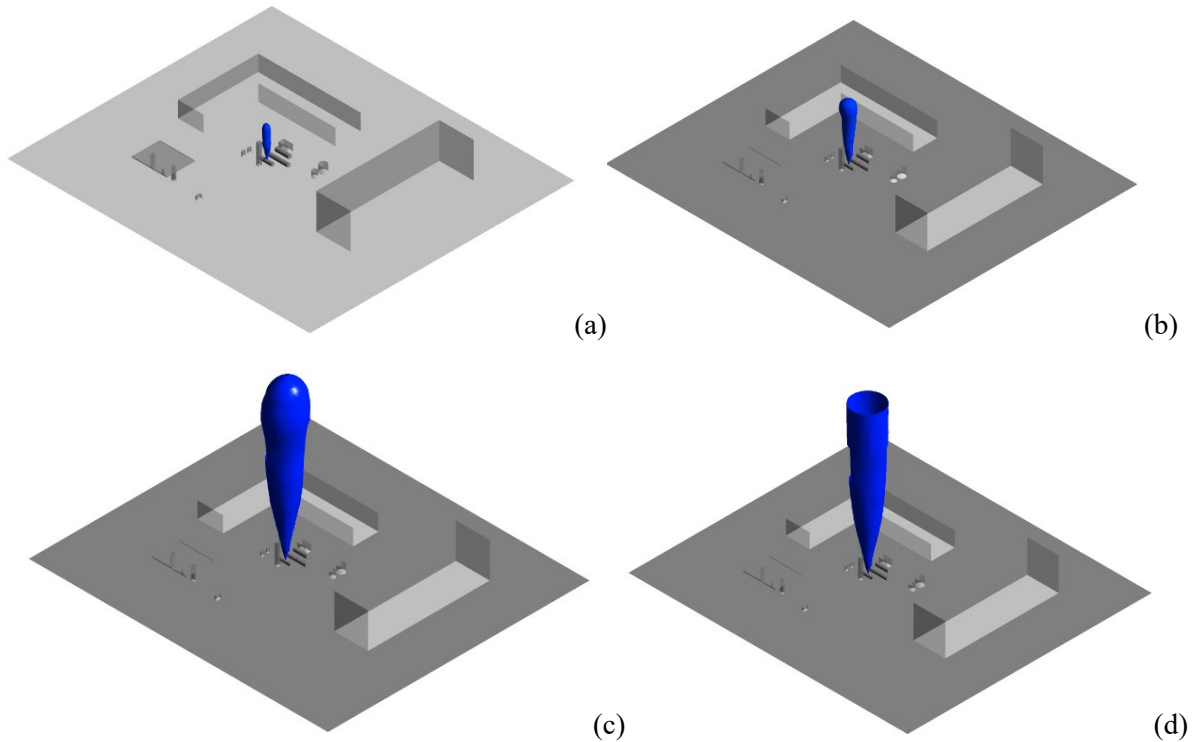
Fig.7 The distribution range of flammable hydrogen cloud when the vertical leakage time is (a) 0.2s, (b) 1s, (c) 10s and (d) 30s.

As the diffusion continues, hydrogen diffuses to the hydrogen energy plant, as shown in Figure 6 (c) - (d). Some hydrogen will continue to diffuse forward along the side walls of the plant, while the other part of hydrogen will be hindered by the wall surface of the plant and diffuse freely along the wall surface. Due to air and wall surface resistance, the diffusion rate of hydrogen gradually decreases. At 10s, the horizontal forward velocity dissipates to a very low level, forming a partial spherical aggregation region at the boundary at 10s. At this time, buoyancy and free diffusion drive dominate, and hydrogen begins to diffuse upward.

3.1.2 Vertical leakage of 45MPa hydrogen storage tank

When leakage occurs at the leakage port on the upper wall of the hydrogen storage tank, hydrogen will leak vertically from the leakage port. The flammable hydrogen cloud changes with time during the leakage process, as shown in Figure 7. The direction of hydrogen leakage is vertical and upward, with a wind speed of 0 m/s in the environment. High-pressure hydrogen rapidly rises from the leakage location and spreads around. As the height increases, the flammable hydrogen cloud takes on a shape that is thick above and thin below. A spherical region appears at the top of the flammable hydrogen cloud, continuously moving upward over time. This is because as the hydrogen rises, the top hydrogen will lose speed due to the obstruction of air. In contrast, the subsequent hydrogen leakage will rise rapidly, pushing the hydrogen in the top area to continue rising. When the leakage occurred for 30 s, the rise height of hydrogen gas exceeded the entire calculation domain.

When the leakage lasts for 10 seconds, the flammable hydrogen cloud has already spread to the boundary of the computational domain, reaching a height of 76 meters. Therefore, when the leakage lasts for 30 seconds, the height of the flammable hydrogen cloud is much higher than 80 meters. At 60 m, the hydrogen cloud reaches a maximum width of about 17 m.

3.2 Mass flow rate of hydrogen leakage

The hydrogen leakage rate also significantly impacts the leakage and diffusion of hydrogen. To explore the impact of hydrogen leakage rate on hydrogen leakage and diffusion, four different leakage mass flow rates, namely 1.5589 kg/s, 2.5589 kg/s, 3.5589 kg/s, and 4.5589 kg/s were set up. The size diagram of flammable hydrogen cloud after the same leakage time under different leakage mass flow rates is shown in Figure 8.
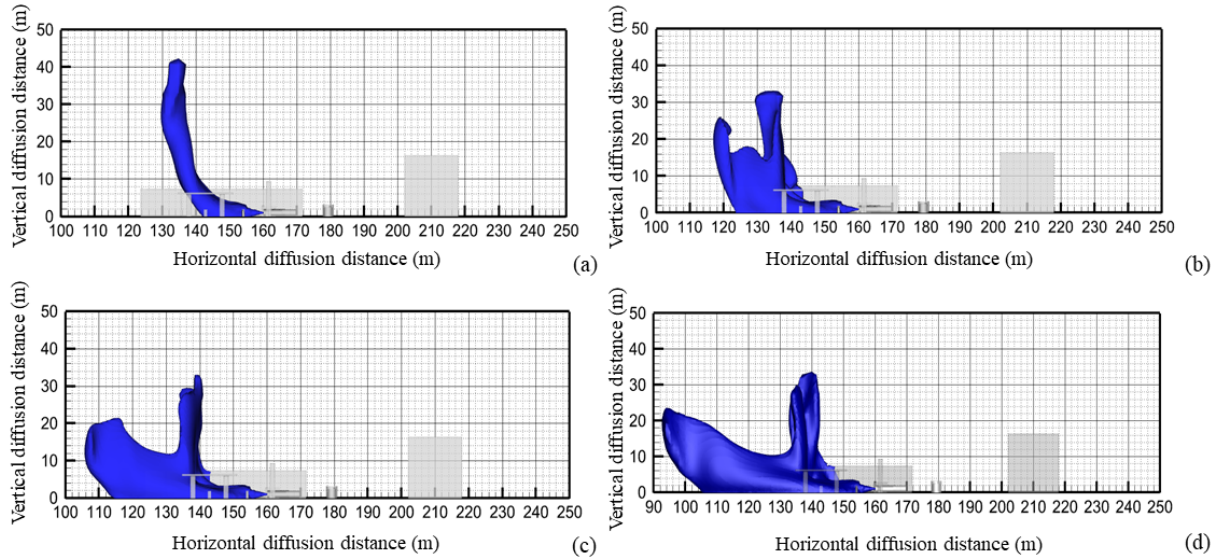

Fig.8 Size diagram of flammable hydrogen cloud after 30 s of hydrogen leakage when mass leakage rates are (a)1.5589kg/s, (b)2.5589kg/s, (c)3.5589kg/s, and (d)4.5589kg/s

It can be seen that the higher the mass flow rate, the farther the horizontal diffusion distance of the flammable hydrogen cloud along the leakage direction and the more the flammable cloud is close to the ground. After 30 s of leakage at different leakage mass flow rates, the diffusion distance and flammable gas cloud volume in each direction are shown in Table 1.

Table 1. Hydrogen diffusion results under different leakage mass flow rates

Mass flow rate	Horizontal diffusion distance	Vertical diffusion distance	Volume of flammable hydrogen cloud
1.5589 kg/s	30.417 m	42.41 m	2277.48 m^3
2.5589 kg/s	43.092 m	33.13 m	3664.88 m^3
3.5589 kg/s	54.283 m	33.08 m	4876.71 m^3
4.5589 kg/s	67.2 m	34 m	6140.46 m^3

According to Table 1, when the leakage mass flow rate increases from 1.5589 kg/s to 4.5589 kg/s, the horizontal diffusion distance increases from 30.417 m to 67.2 m. This is because the amount of hydrogen leaked per unit of time increases as the mass flow rate increases. Driven by pressure, the horizontal diffusion distance of the flammable hydrogen cloud increases, and the volume of the flammable cloud also increases as the mass flow rate increases, from 2277.48 m3 to 6140.46 m3. When the mass flow rate is 1.5589 kg/s, the vertical diffusion distance is the highest, at 42.41 m. When the mass flow rate is 2.5589 kg/s, 3.5589 kg/s, and 4.5589 kg/s, the vertical diffusion distance has no significant difference, ranging from 33 to 34 m. This is because when the mass flow rate is 1.5589 kg/s, hydrogen has not yet leaked to the surface of the hydrogen plant but has begun to diffuse upward under the action of buoyancy. At this time, the velocity loss is small, while under other mass flow rates, hydrogen leaks to the surface of the hydrogen plant and then begins to diffuse upward under the action of buoyancy. Due to the obstruction of the wall surface, the velocity loss of hydrogen at the wall surface is large, and the vertical diffusion amplitude of hydrogen in this part is small.

3.3 Ambient wind direction

Due to the complex surrounding environment of hydrogen storage tanks, different wind directions affect hydrogen diffusion behavior after horizontal leakage. To explore the impact of wind directions on the diffusion results of hydrogen leakage, this section sets up four different wind directions, namely, east, west, south, and north, for simulation research. The simulation scenario is a horizontal leakage of a 45 MPa hydrogen storage tank, with a leakage mass flow rate of 4.5589 kg/s, an ambient wind speed of 2 m/s in different wind directions, an ambient temperature of 293 K, and a leakage duration of 30 s. Due to the large calculation domain space, if the wind speed of 2 m/s is directly used for transient calculation, the dissipation of wind speed will make the ambient wind speed field unstable, leading to inaccurate calculation results. To avoid this problem, the steady-state calculation method is used to simulate the ambient wind speed field before conducting the simulation in this section. The transient simulation is conducted under a stable wind speed field.

When the leakage ends in different environmental wind directions, the distribution map of flammable areas is shown in Figure 9. It can be seen from the figure that different environmental wind directions have a certain impact on the shape of flammable hydrogen clouds, especially when the vertical diffusion of hydrogen exceeds that of the hydrogen energy plant. Its diffusion direction is affected by the environmental wind direction and starts to diffuse along the direction of the environmental wind direction. For hydrogen with a height not exceeding that of a hydrogen plant, its leakage and diffusion behavior are less affected by the ambient wind direction, mainly because the hydrogen plant blocks the ambient wind, reducing the wind speed of the part shielded by the hydrogen plant. The diffusion distances in different directions under different wind directions are shown in Table 2.

As can be seen from Table 2, when the wind direction is easterly, the maximum horizontal diffusion distance is 47.19 m. When the wind direction is westerly, the minimum horizontal diffusion distance is 25.02 m. Therefore, the easterly wind will accelerate the horizontal diffusion of hydrogen along the leakage direction, while the westerly wind will hinder the horizontal diffusion of hydrogen along the leakage direction. For vertical diffusion, it can be seen that when the wind direction is upwind, the vertical diffusion of hydrogen is slower, and it will gather near the hydrogen storage tank. Therefore, when the wind direction is upwind, the maximum volume of flammable clouds at the end of leakage is 9419.06 m^3, with the highest risk. When the wind direction is southerly, the wind direction is from south to north, and there are no obstacles during this period. After a leak occurs, the hydrogen diffusion effect is the best, so the minimum flammable zone volume is 8124.44 m^3.

Table 2. Diffusion distance results of flammable hydrogen clouds in different wind directions

Wind direction	Horizontal diffusion distance	Vertical diffusion distance	Volume of flammable hydrogen clouds
East wind	47.19 m	32.91 m	9160.21 m^3
West wind	25.02 m	28.76 m	9419.06 m^3
South wind	30.61 m	40.12 m	8124.44 m^3
North wind	41.93 m	39.22 m	9251.27 m^3

3.4 Ambient wind speed

The previous section studied the impact of different wind directions on hydrogen leakage and diffusion after an accident in a 45 MPa hydrogen storage tank. This section will explore the impact of wind speed on hydrogen leakage and diffusion. The design reference ambient wind speeds are 2 m/s, 5 m/s, 8 m/s, and 10 m/s. Due to the large computational domain space, if wind speed is directly used for transient calculations, the dissipation of wind speed will make the environmental wind speed field unstable, resulting in inaccurate calculation results. To avoid this issue, before conducting the simulation, use steady calculation methods to simulate the environmental wind speed field, and conduct transient simulation under a stable wind speed field. The study of wind direction in the previous section shows that when the wind direction is upwind, flammable clouds will gather between the hydrogen storage

area and the hydrogen energy plant, with a high risk. Therefore, the wind direction in this section is selected as the upwind direction. The west wind and other conditions are the same as those in Section 3.2. The size diagram of flammable hydrogen clouds under different wind speeds is shown in Figure 10.

It can be seen from the figure that the ambient wind speed has a significant impact on the diffusion behavior of hydrogen after leakage from the hydrogen storage tank. As the wind speed increases, the flammable hydrogen clouds gradually moves toward the storage tank area, especially the hydrogen that diffuses to high places. Due to the loss of speed, it is more likely to be affected by the wind speed and move in the reverse leakage direction. Due to the small number of obstacles near the hydrogen storage area, hydrogen at high altitudes will accelerate its diffusion due to the impact of ambient wind. The results show that the higher the wind speed, the lower the height of flammable clouds and the smaller the volume of combustible clouds. The diffusion distances and volumes of combustible hydrogen clouds in various directions under different wind speeds are shown in Table 3.

It can be seen from the table that as the wind speed increases, the vertical diffusion distance gradually decreases. In contrast, the horizontal diffusion distance along the leakage direction does not decrease. The main reason is that when the wind speed reaches a certain value, a backflow will form on the side wall of the hydrogen plant, accumulating hydrogen on the side wall to form a flammable zone, thereby increasing the horizontal diffusion distance along the leakage direction.

Table 3. Diffusion distance results of flammable hydrogen clouds in different wind speed

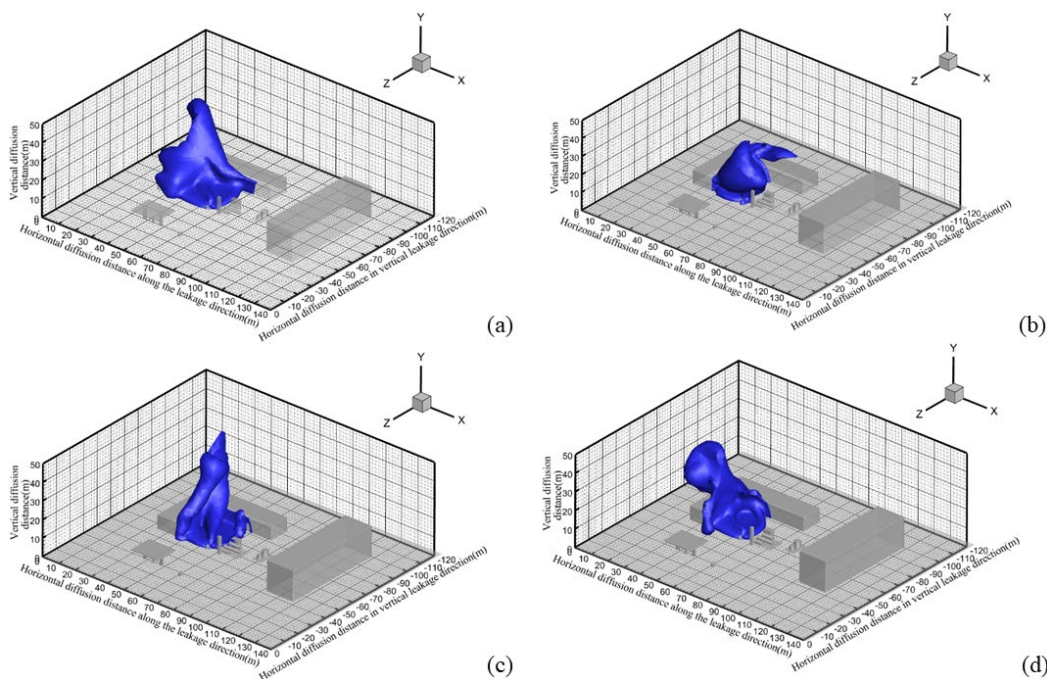| Wind speed	Horizontal diffusion distance	Vertical diffusion distance	Volume of flammable hydrogen clouds
2 m/s	25.02 m	28.76 m	9419.06 m^3
5 m/s	29.59 m	18.799 m	8259.45 m^3
8 m/s	35.843 m	15.58 m	6568.19 m^3
10 m/s	36.423 m	15.14 m	5738.24 m^3

Fig.9 Size diagram of flammable hydrogen clouds during horizontal leakage of 45 MPa hydrogen storage tank for 30 s with wind directions of (a) east wind (X-axis negative direction), (b) west wind (X-axis positive direction), (c) south wind (Z-axis negative direction) and (d) north wind (Z-axis positive direction)
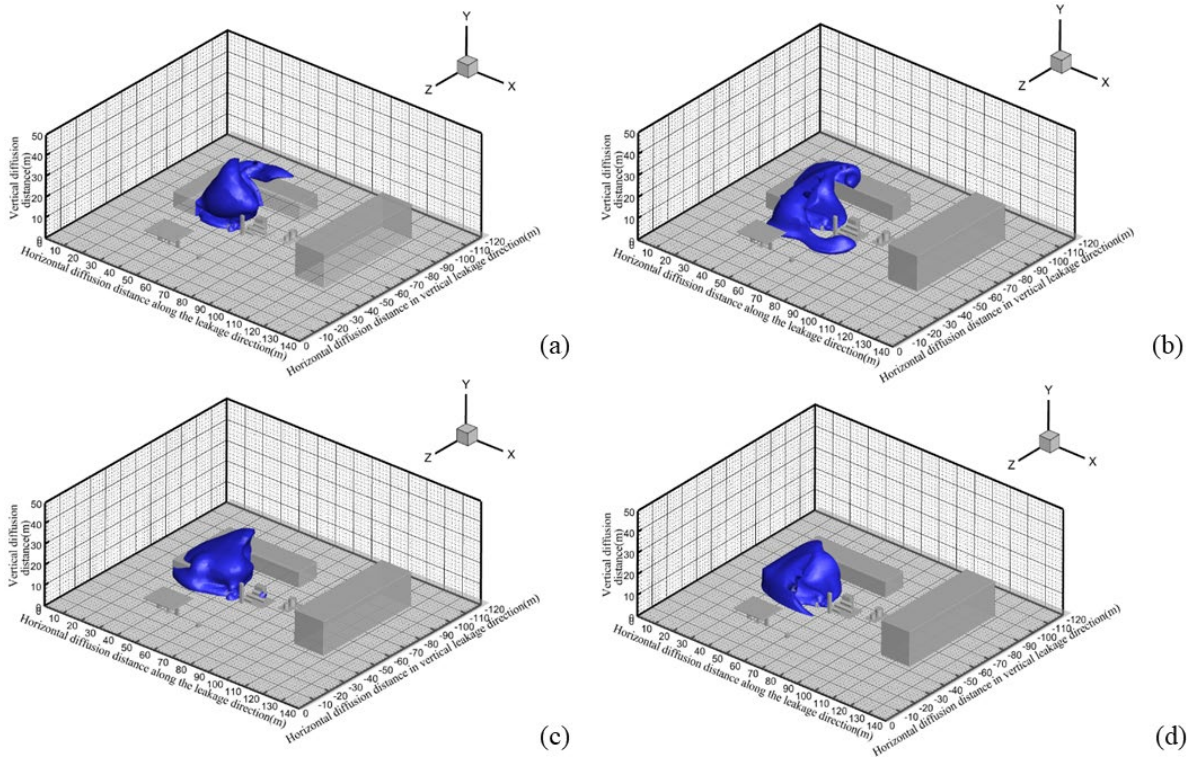
Fig.10 Size diagram of flammable hydrogen clouds after 30 seconds of hydrogen leakage at wind speeds of (a) 2m/s, (b) 5m/s, (c) 8m/s, and (d) 10m/s

4. PREDICTION OF HORIZONTAL DIFFUSION DISTANCE AND VERTICAL DIFFUSION DISTANCE BASED ON ARTIFICIAL NEURAL NETWORK MODEL

The simulation analysis of the third section explored the impact of different factors on the hydrogen diffusion distance when a horizontal leakage occurs in a 45 MPa hydrogen storage tank. It is necessary to accurately predict the horizontal and vertical diffusion distance of combustible hydrogen clouds in hydrogen leakage accidents. BP artificial neural networks had been proven to have good accuracy and speed advantages in predicting results [12]. Therefore, this section established a BP neural network model to predict the diffusion distance of flammable hydrogen clouds. This study used the mass flow rate of hydrogen leakage, ambient wind speed, and hydrogen leakage time which have a significant impact as input parameters for the neural network model. The wind direction is set to the most dangerous wind direction, that is, from west to east. The output values of the neural network are the horizontal diffusion distance and the vertical diffusion distance.

4.1 Establishment and Training of BP Artificial Neural Network

When building a BP artificial neural network, the number of neurons in the hidden layer is set to 8, the number of hidden layers is selected to 1, and the number of neurons in the input, hidden, and output layers is 3, 8, and 2, respectively. The hidden and the output layers adopt different activation functions, namely *tansig* and *purelin*. All 240 sets of data were from the simulated operating conditions in Part III, with the same leakage rate. All data were randomly allocated into training sets, validation sets, and test sets in a 6:2:2 ratio. Figure 10 shows the regression coefficient diagrams and the values of the correlation coefficient R between the target value and the predicted value in different processes after the test is completed.

The correlation coefficient R values during training, validation, and testing are 0.97538, 0.97862, and 0.98292, and the correlation coefficient R for the entire process is 0.97707. It can be seen that the established BP artificial neural network captures the correlation between three input parameters (leakage

mass flow rate, ambient wind speed, and hydrogen leakage time) and the target value (horizontal diffusion distance and vertical diffusion distance). Therefore, the BP artificial neural network established in this study can be used to predict horizontal and vertical diffusion distance of flammable hydrogen clouds after a leakage accident occurs in this system.

4.2 Neural Network Optimization Based on Sparrow Search Algorithm (SAA)

Although the BP neural network is widely used in a variety of scenarios, it still has certain defects. When the network is initialized with different initial weights, the neural network will converge to a local minimum. And when the error gradient is relatively flat, it will cause the network to converge slowly or even not converge. Therefore, this section uses the SAA [13] to optimize the built BP neural network to improve the prediction accuracy.

The correlation coefficient R values of the neural network optimized using SAA during training, testing, and validation are 0.99491, 0.99372, and 0.99452, respectively, and the overall correlation coefficient R is 0.99418. The correlation coefficient R-values of the four processes are higher than that of the BP artificial neural network before optimization, indicating that the BP artificial neural network optimized using the SAA has a better correlation.

In order to better analyze the predictive performance of the neural network before and after optimization, the horizontal and vertical diffusion distances predicted by the artificial neural network before and after optimization were compared with the actual values. In this process, three indicators, namely, mean absolute error (MAE), mean absolute percentage error (MAPE), and mean square error (MSE), are mainly used. The error comparison of the results before and after the final optimization is shown in Table 4 and Table 5.

As can be seen from Table 4, for the prediction of horizontal diffusion distance, the MAE between the prediction result of the optimized BP artificial neural network and the actual value is 1.6367 m, MSE is 6.4573%, and MAPE is 9.7864%. However, the MAE between the prediction result of the optimized BP artificial neural network and the actual value is 0.4991 m, MSE is 2.7818%, and MAPE is 2.4801%. According to the above results, compared to the previous optimization, the optimized BP artificial neural network achieves better results in predicting horizontal diffusion distance. Combining the information in Table 5, it can be seen that for the prediction of vertical diffusion distance, the MAE between the prediction result of the optimized BP artificial neural network and the true value is 1.2924 m, MSE is 5.3698%, and MAPE is 6.6092%. However, the MAE between the prediction result of the optimized BP artificial neural network and the true value is 0.1698 m, MSE is 1.0871%, and MAPE is 1.9337%. Similarly, the error indicators of the SAA-BP artificial neural network are lower than those of the BP artificial neural network. In summary, the prediction effect of the BP artificial neural network model optimized using the sparrow search algorithm on the horizontal and vertical diffusion distances of flammable hydrogen clouds is improved compared to the BP artificial neural network model before optimization.

Table 4. Comparison of model evaluation indicators before and after optimization (horizontal diffusion distance prediction)

Model	MAE	MAPE	MSE
BP-ANN	1.6367	9.7864%	6.4573%
SAA-BP-ANN	0.4991	2.4801%	2.7818%

Table 5. Comparison of model evaluation indicators before and after optimization (vertical diffusion distance prediction)

Model	MAE	MAPE	MSE
BP-ANN	1.2924	6.6092%	5.3698%
SAA-BP-ANN	0.1698	1.9337%	1.0871%

5. CONCLUSION

In this paper, a computational fluid dynamics simulation analysis of hydrogen leakage and diffusion was conducted for a hydrogen refuelling station. The BP artificial neural network model was established to predict the horizontal and vertical diffusion distances of flammable hydrogen clouds after leakage. The neural network model was optimized using the sparrow search algorithm, and the prediction effects before and after optimization were compared. The main conclusions are as follows:

(1) A three-dimensional simplified model of an open space hydrogen refuelling station was established. The diffusion behavior of hydrogen at different locations of a 45MPa hydrogen storage tank was analyzed, and a parameter study was conducted on the horizontal leakage of the 45MPa hydrogen storage tank, including the leakage mass flow rate, wind direction, and wind speed. The research shows that the greater the mass flow rate, the farther the diffusion distance of hydrogen in the horizontal direction is; The wind direction will lead to a wider diffusion range of the flammable hydrogen cloud in the wind direction. When the environmental wind direction is opposite to the leakage direction, the risk is highest; Wind speed can affect the horizontal and vertical diffusion distances of leaked hydrogen.

(2) A BP neural network was established to predict the horizontal and vertical diffusion distances of the flammable cloud during leakage accidents, and the sparrow search algorithm was used to optimize the BP neural network. The results show that the correlation coefficients of the three processes of BP neural network training, validation, and testing before optimization are 0.97538, 0.97862, and 0.98292. The correlation coefficients of the three processes of the BP artificial neural network after optimization are 0.99491, 0.99372, and 0.99452, respectively, which are higher than those before optimization. Moreover, the average absolute errors between the horizontal and vertical diffusion distances of the flammable hydrogen cloud predicted by the optimized BP artificial neural network and the actual values were only 0.4991 m and 0.1698 m, MSE decreased from 6.5473% and 5.3698% before optimization to 2.7818% and 1.0871%, and MAPE decreased from 9.7864% and 6.6092% to 2.4801% and 1.9337%. In summary, SAA-BP artificial neural network has a better effect on predicting the horizontal and vertical diffusion distances of flammable hydrogen clouds.

ACKNOWLEDGMENT

REFERENCES

[1] Qian, J.Y., Li, X.J., Gao, Z.X., et al. A numerical study of hydrogen leakage and diffusion in a hydrogen refueling station, *International Journal of Hydrogen Energy*, **45**, No.28, 2020, pp. 14428-14439.

[2] Jiao, M.Y., Zhu, H.R., Huang, J.L., et al. Numerical simulation of hydrogen leakage and diffusion process of fuel cell vehicle. *World Electric Vehicle Journal*, **12**, No.4, 2021.

[3] Kim, E., Park, J., Cho, J.H., et al. Simulation of hydrogen leak and explosion for the safety design of hydrogen fueling station in Korea. *International Journal of Hydrogen Energy*, **38**, No.3, 2013, pp. 1737-1743.

[4] Liang, Y., Pan, X.M., Zhang, C.M., et al. The simulation and analysis of leakage and explosion at a renewable hydrogen refuelling station. *International Journal of Hydrogen Energy*, **44**, No.40, 2019, pp. 22608-22619.

[5] Rigas, F., Sklavounos, S. Evaluation of hazards associated with hydrogen storage facilities. *International Journal of Hydrogen Energy*, **30**, No.13-No.14, 2005, pp. 1501-1510.

[6] Worster M G., Huppert H E. Time-dependent density profiles in a filling box. *Journal of Fluid*, 132, 1983, pp. 457-466.

[7] Denisenko V P., Kirillov I A., Korobtsev S V., et al. Hydrogen-air explosive envelope behavior in confined

space at different leak velocities, 2009.

[8] De Stefano M., Rocourt X., Sochet I., et al. Hydrogen dispersion in a closed environment. *International Journal of Hydrogen Energy*, **44**, No.17, 2019, pp. 9031-9040.

[9] Pitts W M., Yang J C., Blais M., et al. Dispersion and burning behavior of hydrogen released in a full-scale residential garage in the presence and absence of conventional automobiles. *International Journal of Hydrogen Energy*, **37**, No.22, 2012, pp. 17457-17469.

[10] Ba Q X., Zhao M B., Zhao Z Y., et al. Modeling of high pressure hydrogen jet fires. *Journal of Tsinghua University (Science and Technology)*, **62**, No.2, 2022, pp. 303-311.

[11] Molkov V, Makarov D, Bragin M. Physics and modelling of under-expanded jets and hydrogen dispersion in atmosphere. *Physics of Extreme State of Matter*, **11**, No.6, 2009, pp. 143-145.

[12] Wang R, Chen B, Qiu S, et al. Comparison of machine learning models for hazardous gas dispersion prediction in field cases. *Int J Environ Res Public Health*, **15**, No.7, 2018, 1450.

[13] Xue J K, Shen B. A novel swarm intelligence optimization approach: sparrow search algorithm. *SYST SCI CONTROL ENG*, **8**, No.1, 2020, pp. 22-34.